BIOMECHANICS & BIOMEDICAL ENGINEERING

National Technical University of Athens

Technical Report

LOW COST FORCE SENSOR

Team members:
Gartzonikas Dimitrios
Tzortzopoulos Georgios

Mentor: Gκousioudi Anastasia Consultant: Tzeranis Dimitrios

Milestone 1: Electronic interface design

Design Objective

The objective of the following project is to design and finally build a device designed around a Force Sensitive Resistor (FSR sensor) that will be able to measure force values applied on test specimens, ensuring the low cost of the final design.

More specifically, the aim is to pair the changes in the electrical resistance of the sensor (due to the applied forces intended to be measured) with proportionate voltage changes in the output of the electronic interface. The device will then be calibrated in order to translate the measured output voltage into corresponding force values.

Brainstorming on the definition of the first requirements/evaluation criteria of our system, in the early conception stage, resulted in the following:

1. Good response characteristics
2. Low cost of system
3. Compatibility of available components
4. Ease of assembly
5. Evaluation of noise contribution to the output signal
6. Definition of accuracy of the low force sensor system
7. Definition of sensitivity of the system
8. Definition of distinctive ability of the system
9. Calibration of the system

Analog Electronics Used

The available key electronic components of the circuit were:

- FSR 400 Series Round Force Sensing Resistor

- 12-Bit, 4-Channel Serial Output Sampling Analog-to-Digital Converter (ADS7841)

- OPAx228 (High Precision, Low Noise Operational Amplifier)

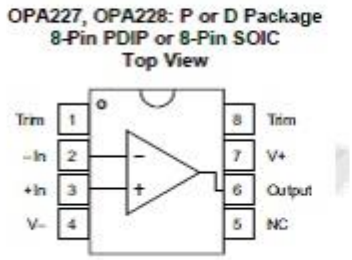

- REF02 Voltage Reference

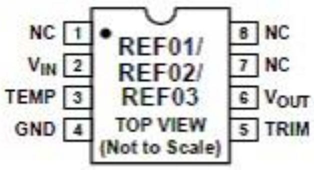

- µA79M00 Series Negative-Voltage Regulator

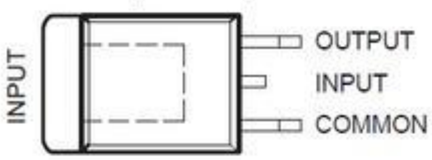

- Any additional resistor and capacitor parts necessary

More details about the Force Sensor

A force-sensing resistor (FSR) is a material whose resistance changes when a force or pressure is applied. These devices are fabricated with elastic material in four layers, consisting of:

- A layer of electrically insulating plastic;
- An active area consisting of a pattern of conductors, which is connected to two leads on the tail of the sensor;
- A plastic spacer, which includes an opening aligned with the active area, as well as an air vent through the tail;
- A flexible substrate coated with a thick polymer conductive film or ink, aligned with (or printed on) the active area.

In general, a FSR sensor is a piezo-resistivity conductive polymer, which changes resistance in a predictable manner following application of force to its surface. The sensing area consists of both electrically conducting and non-conducting particles suspended in a matrix. The particle sizes are of the order of fraction of microns, and are formulated to reduce the temperature dependence, improve mechanical properties and increase surface durability. Applying a force to the surface of the sensing film causes particles to touch the conducting electrodes, changing the resistance of the film.

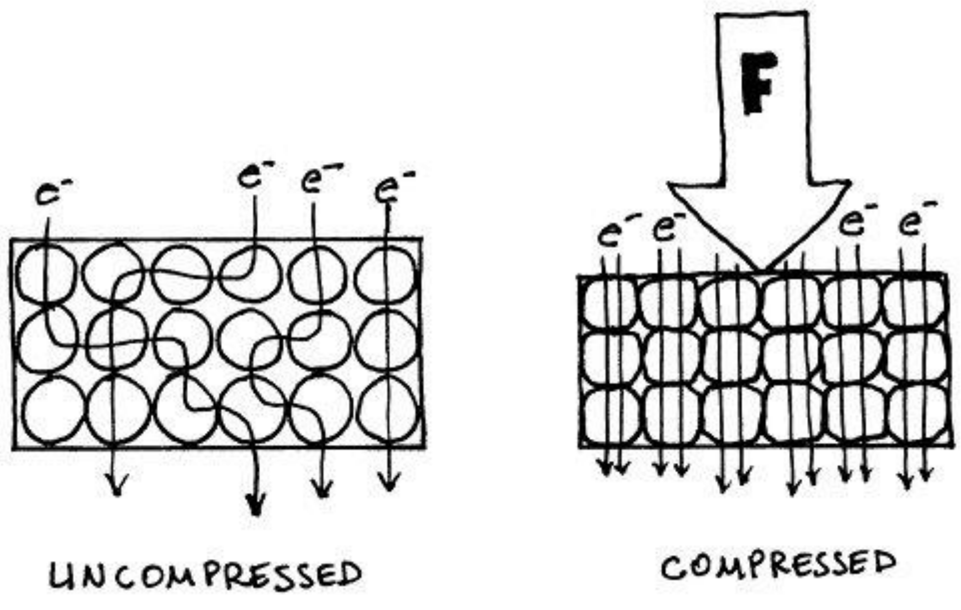

Because the FSR's operation is dependent on its deformation, it works best when affixed to a support that is firm, flat, and smooth. Mounting the sensor on a curved surface (as is often the case when placing sensors on the body or clothing, especially on applications such as a dataglove) reduces measurement range and resistance drift. One solution is to use a sensor with a smaller active area, since less of the sensing area will be deformed by the contours of

the body. In our case this problem was partially solved with the use of rubber discs (for more details, see "Measuring FSR's Resistance").

Bending the tail will also affect the performance of the FSR as the deformed air vent of the sensor's tail will change the pressure conditions inside the sensor's cavity. In cases where bending the sensor cannot be avoided, a preliminary calibration is strictly necessary to assure consistent results. Special care was taken during the calibration of our layout to immobilize our FSR in order to avoid such problems. Moreover the tail is also relatively fragile, and if bent far enough the conductive leads inside it will break, rendering the sensor useless and difficult to repair.

The FSR's output signal is a monotonic function of area and pressure. When enough force is applied, this function changes slope quickly due to sensor saturation. After this point output will not be significantly affected by an increase in applied pressure.

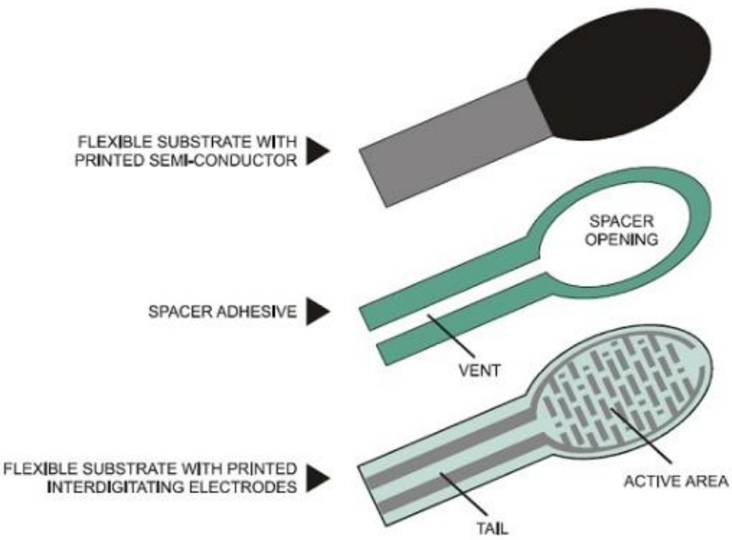

Preliminary Design of Analog Electronics

The operational manuals of the available components provided us with a great number of layout alternatives, covering a variety of practical applications with according layout suggestions. This gave us the opportunity to come up with a series of alternative approaches to the problem of the amplification of our sensor's signal. However, we chose a simple buffer configuration as our starting point, as suggested by the force sensor manufacturer. The basic concept is shown below:

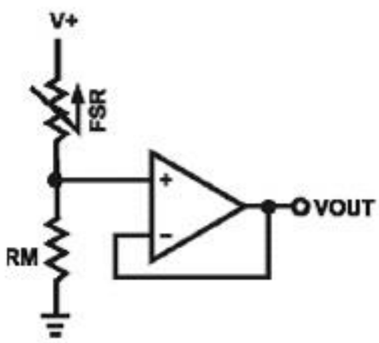

The FSR works as a variable resistor in a voltage divider configuration, providing us with a variable voltage, proportional to the conductivity shift of the Sensor. The buffer isolates the circuit's output from our reference voltage and generally reduces the interaction between the circuit amplification circuit and the rest of the final measurement device components.

We have tried out some alternative layouts, in an effort to best match our design criteria. Some of the suggested layouts can be seen bellow:

- **Bridge connection layout:**

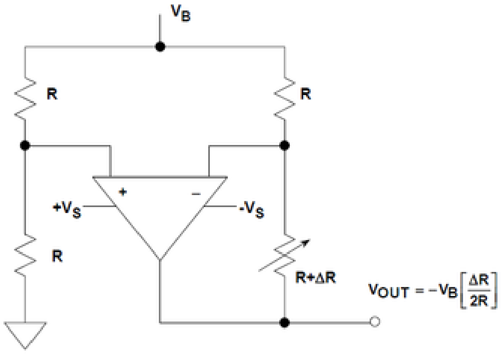

- **Inverting amplifier layout:**

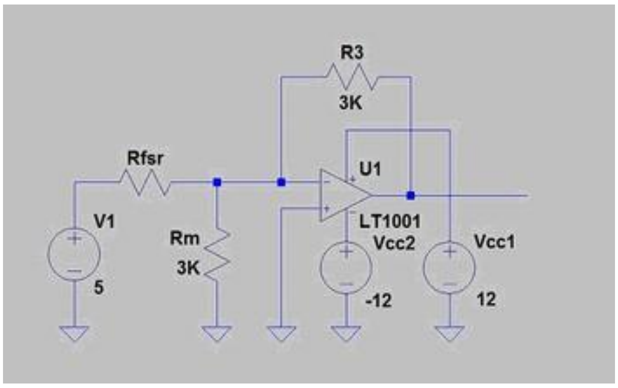

Evaluation and Final Approach

After designing and simulating the operation of the various proposed designs in the LTSpice and Tina-TI simulation environments (SPICE-based programs that simulate the operation of electronic circuits) we discarded those layouts that didn't meet our restricting criteria as defined by the available components. Our specifications regarded:

- Keeping the output of our amplification circuit in the 0-5 Volts range, as defined by the operational range of our analog-to-digital converter;
- Isolating the amplification subsystem of our measurement device from the rest of its components;
- Keeping our output signal as linear as possible in the measurement range, so as to ensure the optimal use of our measured force range;
- Keeping the components number as low as possible - lowering the device's cost
- Simplifying the electric supply requirements of the final device.

The most suitable alternative for amplifying the sensor's signal proved to be a simple non-inverting opamp configuration. Its gain capabilities, low number of components and low impedance of the opamp's output simplified the practical issues that occur on similar applications.

The preliminary schematic of the final system layout (the LT1001 operational amplifier is random choice here) is shown below in its simplest form (a buffer configuration):

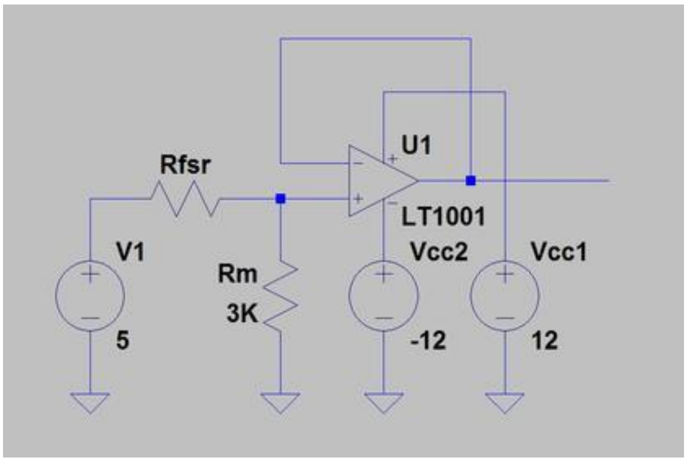

In the picture above are shown the V1 voltage supply (corresponding to the input voltage reference, as provided by our REF02), our FSR sensor (simulated by the variable resistor Rfsr), the voltage divider layout that carries our FSR and a reference resistance (of predetermined value - Rm) that defines the response of our device in relation to Rfsr/Rm, the feedback loop of the operational amplifier that connects its output with its inverting input, and finally the necessary voltage supplies for our op amp (Vcc).

Suggested Features:

Due to the special characteristics of the sensor (nonlinear correlation of force and conductivity, suggested high sensitivity for low force values/low sensitivity for high force values etc.), we considered the possibility of including a number of features to the original design, so as to increase the efficiency of our device for different measuring conditions. The most promising of the suggested features are shown in the following schematic, representing an advanced version of our preliminary design:

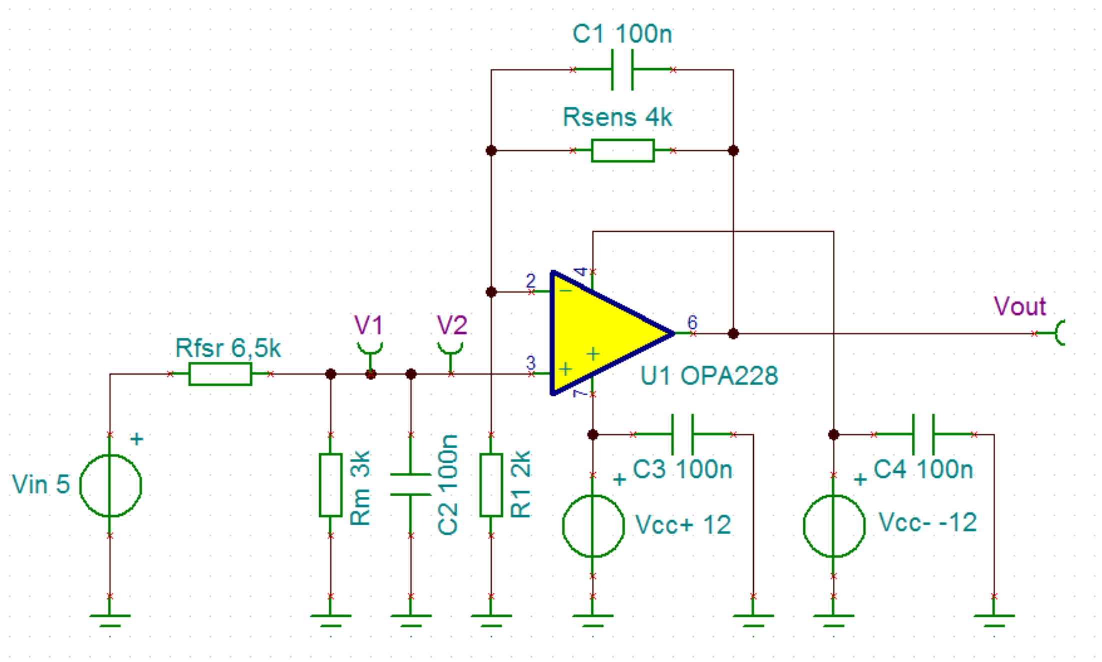

Sensitivity Switch (Rsens):

As seen on the diagram below (manufacturer's manual), the force sensor doesn't have the same response for the whole force range, with one of the factors it is dependent to being the value of the voltage divider's reference resistance (Rm). In order to increase the distinctive ability of our circuit for smaller force values, we considered the potential use of an adjustable gain pot or a variable gain selector that would increase the linear gain of our amplifier circuit. The position of the mentioned switch is on the feedback loop of the amplifier (represented by the Rsens resistance in the schematic above).

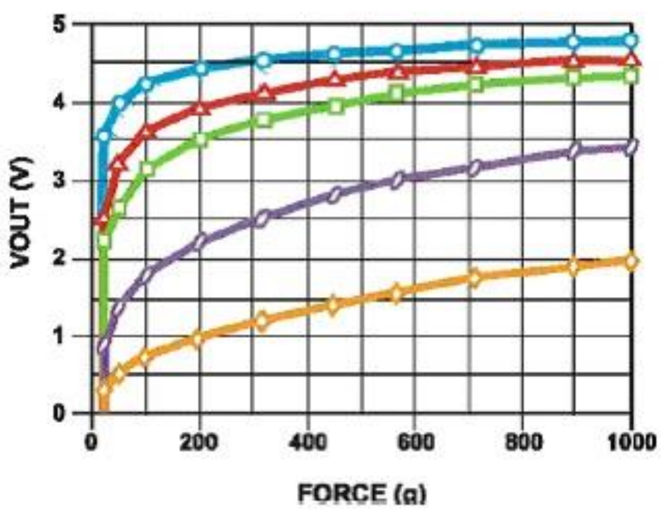

For a more precise approximation of the measured force, we concluded to the use of a rotary switch that moves between four positions, inserting resistors of predetermined value to the feedback loop, each assigned to different predetermined gain values. The circuit's gain corresponds to the relation of Rsens/R1.

From the information that the FSR manufacturer's manual provided, we made a first approximation of the FSR's behavior. The manufacturer's information and the result of our approximation is shown below:

APROXIMATION		
force (g)	$R_{diagram}$ (Ω)	$R_{aproximation}$ (Ω)
0.1	-	1147791.08
20	30000.00	22516.38
50	10000.00	11408.46
100	6000.00	6821.23
250	3300.00	3456.14
500	2000.00	2066.46
1000	1100.00	1235.56
2000	750.00	738.75
4000	450.00	441.71
7000	300.00	291.61
10000	250.00	223.80

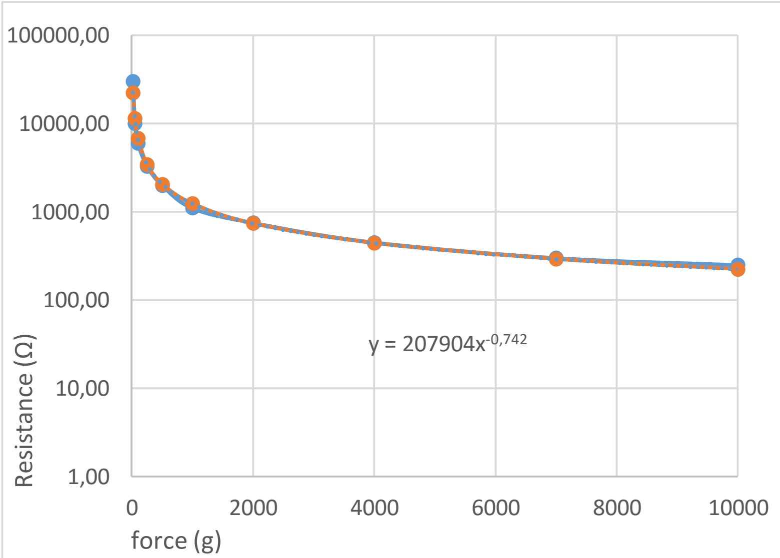

According to our approximation, we decided to define four different gain values (which translates to four different Rsens/R1 ratios) for the following force classes:

- For force values 0-100 g, the gain will be set to 3 (Rsens = 2R1)
- For force values 101-250 g, the gain will be set to 2 (Rsens = R1)
- For force values 251-500 g, the gain will be set to 1.5 (Rsens = R1*1/2)
- For force values greater than 501 g, the gain will be set to 1 (Rsens = 0 = short circuit, practically resulting in a buffer configuration)

Its specific implementation will be examined in relation to the behavior of our sensor as this will be approximated through experimental procedures.

Offset control:

At this point we examined the possibility of zero force values producing non-zero output voltage (including noise or voltage offset caused by unpredictable factors). A suggested solution would be the use of an offset control integrated on the operational amplifier. This would also give us control over measured voltage, giving us the ability to express the measured force in relation to an initial load.

However, this solution (as others) was rejected as the extra components added complexity to our schematic, increasing the number of components and increasing at the same time potential sources of noise in our circuit.

Milestone 2: Implementation

Subsystems, Task Assignment & Subsystem Detailed Design

Below follows the final schematic of our amplification circuit in detail:

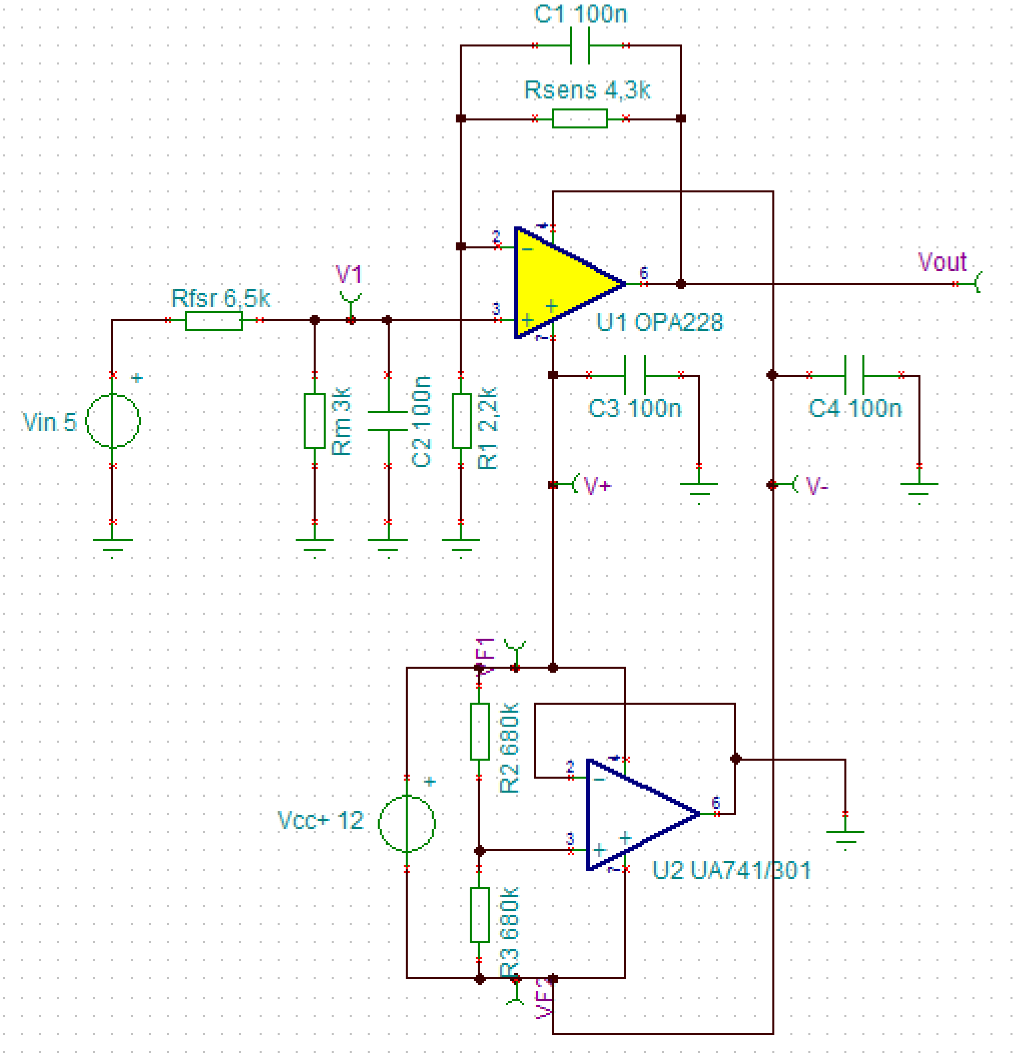

Capacitors:

As seen above, the final schematic includes a number of capacitors that serve different protection purposes. Capacitor C2 forms a low pass filter in series with our circuit's input, protecting our opamp from sudden voltage changes (e.g. voltage spikes from connecting/disconnecting parts of the circuit) and eliminating external high frequency noise that could enter our circuit. Capacitor C1 also protects our system from sudden voltage changes by

adding slight dynamic and phase alterations to the opamp's loop signal, preventing unwanted oscillations that would alter the output of the circuit or even damage our opamp. The decoupling capacitors C3 and C4 are connected to the supply voltages of the amplifier as suggested by the manufacturer. In general, small capacitor values were selected (1μF) so that they contribute to the dynamic response of the system as little as possible.

Voltage Supply Sub Circuit:

Our selected opamp has the ability to run with both a dual supply voltage, and a single positive supply (negative pin in this case corresponds to ground). In the case of dual supply, the values of the negative and positive supply voltage values have to be greater than the intended measured voltage range, in order to keep the amplified signal unaffected. This means that for a measured range of 0-5 Volts we have to power our opamp with a dual supply voltage, making sure that the positive supply is greater than 5 Volts (which is equal to the maximum measured voltage as defined by our analog to digital converter).

The first and most important practical issue that occurred when setting up the supply of our device was the restricted range of positive and negative supply voltages that were available: while we had a big range of robust and accurate positive voltage supplies to choose from, the available negative supplies were not suitable to our application.

A first approach was the implementation of a voltage divider sub circuit, setting the common ground as our middle reference voltage. This would give us the ability to divide a positive voltage supply to intervals suitable for our application (for example we could divide a +12V supply to +8V and a -4V interval). Unfortunately the internal resistance of our opamp made this option impossible to implement.

To cope with this problem, we built a complimentary small voltage supply circuit in order to provide our opamp with the appropriate negative and positive supply voltages. We used a dedicated opamp (UA 741) that is integrated in a voltage divider configuration, powered by a 12V external supply. The two leads of the voltage divider are connected both to the opamp's supply voltage inputs and the supply inputs of the main amplifier circuit. The middle node of the voltage divider is connected to the non-inverting input of the sub circuit's opamp, and its output is connected to the inverting input and the common ground.

The resulting sub circuit splits the provided voltage in a negative and a positive fraction of equal absolute value. The chosen 12V power supply as a result provides the main opamp with a +6V and a -6V supply, giving us the ability to make measurements in a range falling between -4.5V to +4.5 Volts, a range that is acceptable for our application.

Building the Circuit

At this point we started building the amplifying circuit along with the rest of the necessary components. We constructed and assembled the subsystems of the device on a small breadboard because of its flexibility on disassembly and the ease that provides on acquiring measurements on the various stages of our device. The reference voltage of the voltage divider

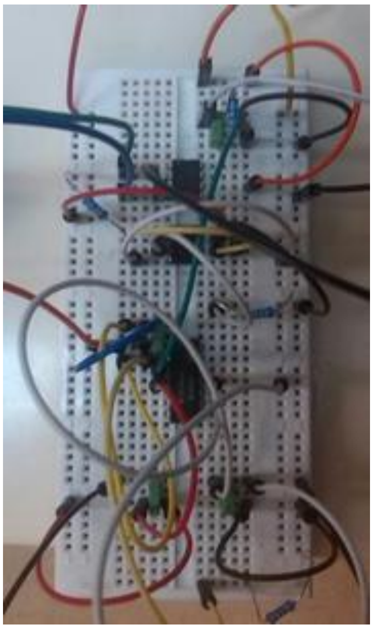

(the input of our FSR) is given by our REF02 which can provide a constant, low noise 5V voltage supply. The resistors' values were chosen as small as possible in order to reduce the chance of extra thermal noise, while at the same time avoiding to disturb their assigned purpose on the various parts of the circuit.

As is, the circuit needs two common 12V power supplies to run: one dedicated supply to power the voltage supply sub circuit and one more to power the VREF and the ADC. These can be either PSUs or any other commercial 12V adapter.

During the construction of the circuit, and before moving on to the evaluation and calibration of the device, we decided to apply some changes that would facilitate the experimental procedures to follow. It has to be noted that the following compromises don't affect the general design of our design in no way.

- We chose to replace the ADC converter with an Arduino. The Arduino's flexibility, programmability and connectivity would make the communication between the device and a portable computer easier, giving us flexibility on a lab's environment.
- We replaced our amplifying opamp with a LM324 opamp so as to protect our original high precision opamp in case of failure.
- Originally we set the amplifying sub circuit on a gain setting of 2. In the course of the experimental procedures we adjusted the gain setting by replacing Rsens with the appropriate Resistance.

Any final minor changes to the design of the device will be decided according to the results of our evaluation and calibration experiments that follow.

Milestone 3: Sensor evaluation and calibration

Measuring FSR's Resistance

The first step was to find out how close are the manufacturer's estimates of the force sensor response to the actual sensor's response. To evaluate the given data we carried out measuring experiments in real conditions. The sensor was put under the penetrator of the load applying machine and was connected with an electronical multimeter in order to measure the resistance value of the sensor for different load values.
Firstly, the need of correct welded connections for the cables came up. Because of the high sensitivity of the sensor that measured even the slightest movements of the cables or bends of the tail, we couldn't repeat the same resistance value measurements for the same applied force. To cope with this problem, we welded the sensor connectors with the cables that drove into the multimeter (and in future applications would be connected to the circuit). The body of the sensor

was and its cables were fastened to the body of the load applying machine in such a way that any unwanted movements were eliminated.

The actuation force of the sensor according to its manufacturer is 0.1 Newton, so our calibration experiments started at 0.1 Newton and continued until we've reached 7.5 Newtons (as defined by the limitations of the load applying machine). The initial load step was 0.002 N/sec and each achieved load was held stable for 30 seconds. After the first two executions of this experiment we made the following observations:

- The force sensor actuated after a load of 0.9 Newtons, something that wasn't at all in compliance with the manufacturer's actuation value;
- The force sensor was not able to verify its recorded resistance through repeated experiments for the same load values.

As mentioned before, on the tip of the sensor are two metal grids that are separated by a conductive polymer. When force is applied to the surface of the sensor, this polymer is compressed and its resistive properties are changed. But due to the unstable performance and high sensitivity of the sensor for small loads (a result of its special structural properties), the varying distribution of the applied force on the surface of the sensor can greatly vary the value of its resistance (it is generally established that FSR sensors have an estimated deviation of 25%). This fact was easily verified after the first repeats of our evaluation experiments.

To cope with this problem, we decided to put the sensor tip between two small discs in order to focus the applied load on the surface of the sensor. Our first choice was to use two bronze discs (6 mm diameter, 2 mm thickness) and the initial experiment was repeated. However the performance of the sensor in this case was totally inconsistent. In order to even out the load distribution on its tip, we tried using two rubber discs of the same size. Below we can see a picture of the discs covering both sides of the sensor:

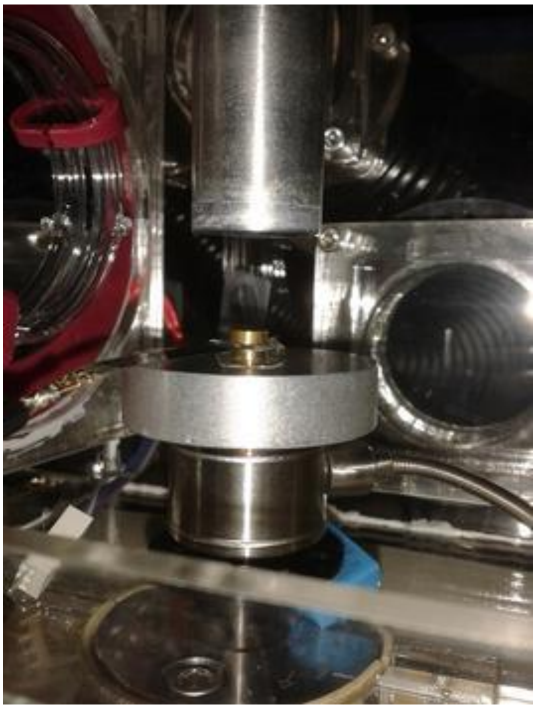

The new layout proved to be more accurate and consistent and so a new experiment protocol was set. Furthermore, because of the load applying machine characteristics it was decided that it is preferable to control the displacement velocity of the penetrator rather than the applied load. The penetrator velocity was set to 0.05 mm/sec and remained for 30 secs at each load level so that the viscoelastic effects of the rubber would calm down. The load range began at 0.1 Newton and continued from 0.5 to 7.5 Newtons in stable steps of 0.5 N. This experiment was repeated nine times in order to obtain reliable data. The detailed results can be viewed below:

step		test 1	test 2	test 3	test 4	test 5	test 6	test 7	test 8	test 9	Average
1	0.10	-	-	-	-	-	-	-	-	-	-
2	0.50	-	-	-	-	-	-	-	-	-	-
3	1.00	-	-	-	-	380	350	-	205	165	275
4	1.50	4000	1000	300	-	270	150	180	135	120	769.375
5	2.00	170	130	135	370	105	100	90	95	80	141.6667
6	2.50	110	105	91	275	77	75	74	80	70	106.3333
7	3.00	62	57	55	103	47	43.5	72	65	60	62.72222
8	3.50	45	45.5	43	66	39	36.5	53	41	40	45.44444
9	4.00	38	33.5	30	46	33	31	36	34	32	34.83333
10	4.50	30.5	26	27	35.5	30.5	28	29	27	25.5	28.77778
11	5.00	27	24	22.5	32	23.5	23.5	26	23.5	23	25
12	5.50		20.5	20	26	21.5	21.5	23.5	22.5	21	22.0625
13	6.00		18.5	18	22	20	19.5	21	19	18	19.5
14	6.50		17.5	17	21.5	18	18	19	17.5	17	18.1875
15	7.00		16	16	19	16	16.5	18	16.5	15.5	16.6875
16	7.50		15	14.5	17.5	15	15.5	16	15	14.5	15.375

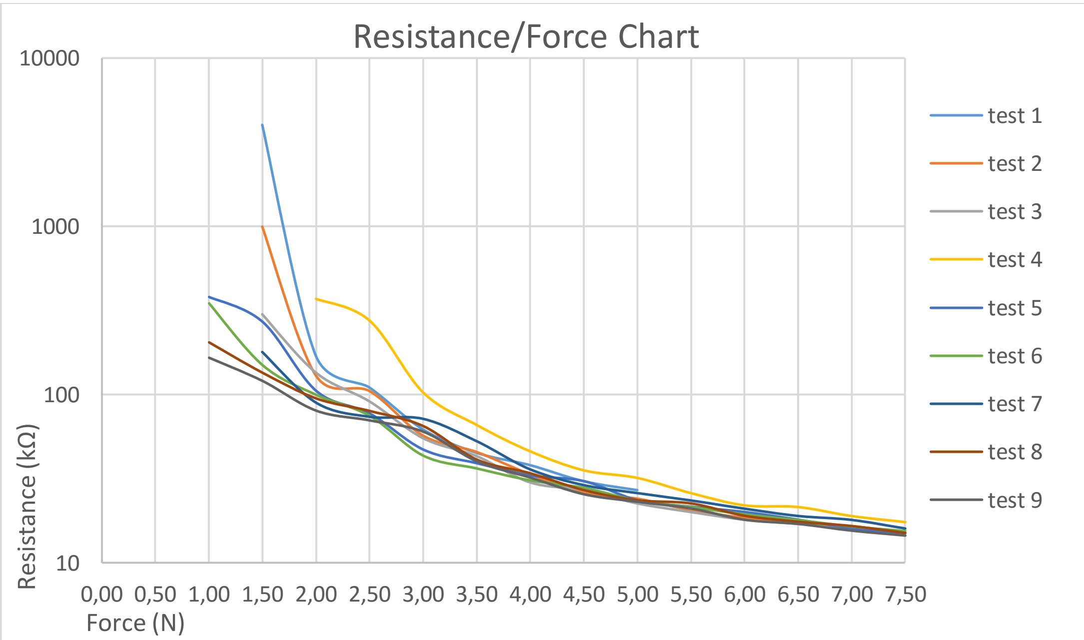

The above measurements resulted in a number of conclusions:

- The measured response doesn't match with the manufacturer's given information
- We have small repeatability, especially for smaller load values
- The measured resistance values have a great deviation on each repetition of the experiment.
- The deviation gets smaller for bigger load values, and the repeatability becomes significant after an applied load of 5 Newtons
- The force sensor actuation load varies between 1 and 2 Newtons

According to this new information, we reproached the operational purpose of our device. The new operational force range is set from 5 to 25 Newtons. The deviation of the measured resistance value is so great that a gain is not necessary on the amplifying circuit of the device, as it will not contribute in the faithfulness of our measurements.

With the new adjustments to our purposed operational conditions, we move on to the final calibration of our device.

Measuring Output Voltage

We connect the finished circuit to our FSR accordingly and its output is connected to the input of our Arduino. The Arduino is then connected via USB to a laptop where we control its sample rate and any other parameters needed through a simple algorithm that documents the given measurements. Those measurements are then stored on a spreadsheet for further analysis.

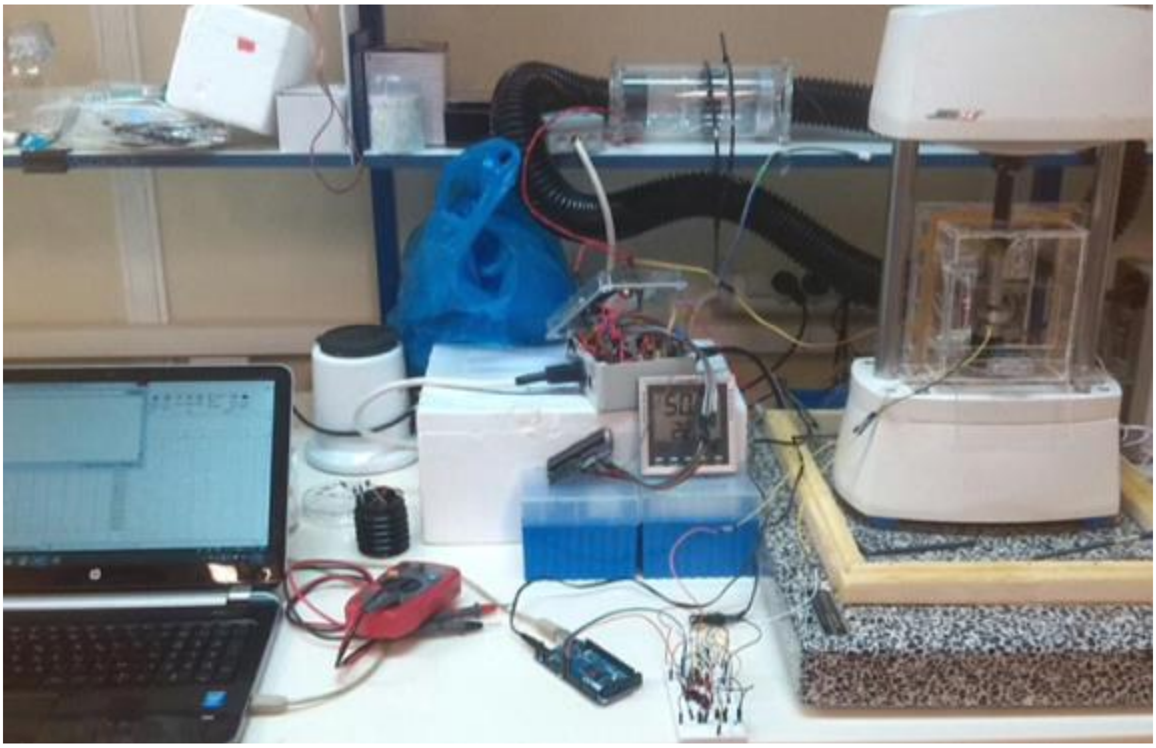

After making sure the measuring system works in the appropriate manner, with the help of our Arduino we take the first measurement on the output of the circuit for an unloaded FSR (which corresponds to 0 Volts on the input of the amplification sub circuit). The measured output is surprisingly 0 Volts, meaning that there is no thermal or electromagnetic noise coming from the various subsystems. From now on, we will assume that noise does not contribute to the results of our measurements.

Once again, the penetrator velocity of the force applying machine was set at 0.05 mm/sec and remained for 30 secs at each load level. The load range was set between 0.1 to 7.5 Newtons as described before. This experiment was repeated 9 more times in order to obtain reliable data.

The plotted graph of the experimental data is shown below:

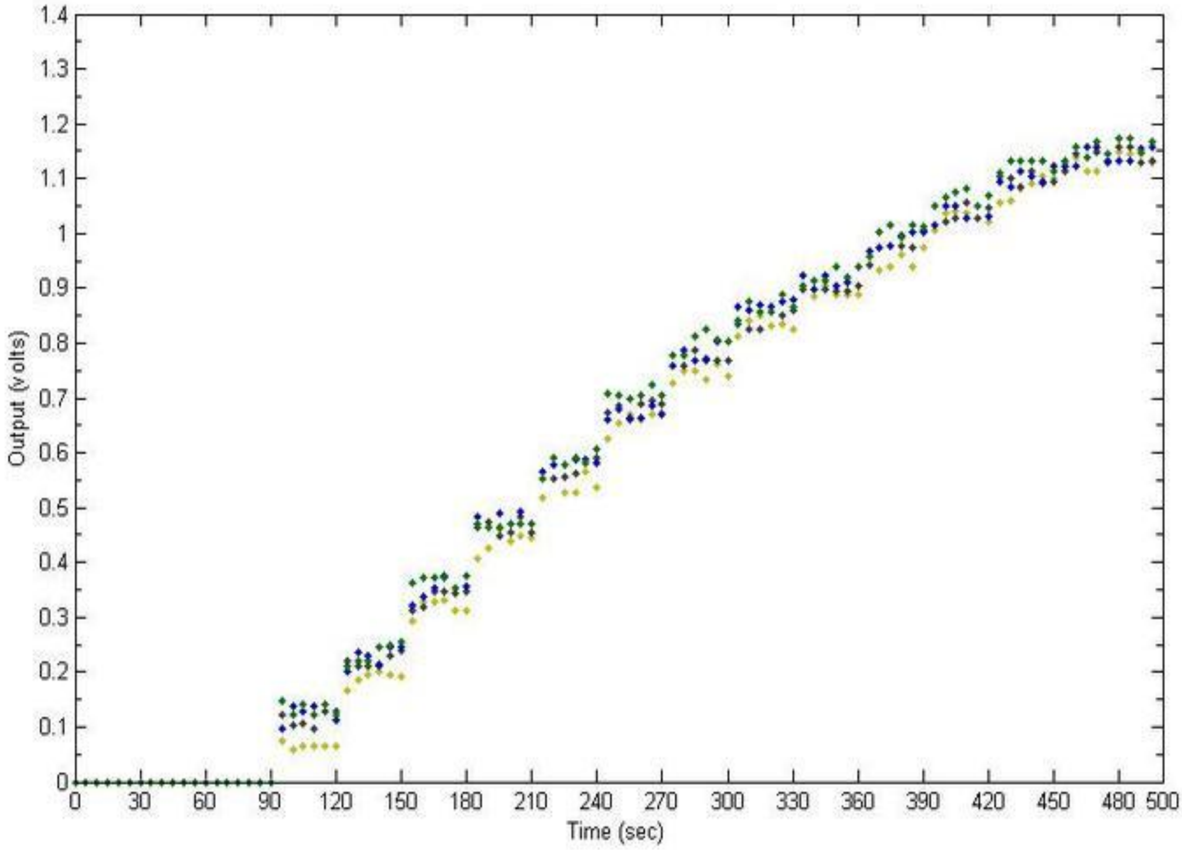

The 30 second intervals correspond to the applied force: (0-30sec=0.1N), (30-60sec=0.5N), (60-90sec=1.0N)... (420-450sec=7.0N), (450-500sec=7.5N)

The experimental results are presented below:

step		test 1	test 2	test 3	test 4	test 5	test 6	test 7	test 8	test 9
1	0.1	-	-	-	-	-	-	-	-	-
2	0.5	-	-	-	-	-	-	-	-	-
3	1.0	-	-	-	-	-	-	-	-	-
4	1.5	0.146628	0.146628	0.146628	0.146628	0.146628	0.073314	0.12219	0.097752	0.146628
5		0.12219	0.12219	0.12219	0.12219	0.12219	0.058651	0.102639	0.136852	0.12219
6		0.14174	0.14174	0.14174	0.14174	0.14174	0.063539	0.107527	0.127077	0.14174
7		0.12219	0.12219	0.12219	0.12219	0.12219	0.063539	0.097752	0.136852	0.12219
8		0.14174	0.14174	0.14174	0.14174	0.14174	0.063539	0.127077	0.14174	0.14174
9		0.12219	0.12219	0.12219	0.12219	0.12219	0.063539	0.127077	0.112414	0.12219
10	2.0	0.210166	0.210166	0.210166	0.210166	0.210166	0.166178	0.219941	0.200391	0.210166
11		0.219941	0.219941	0.219941	0.219941	0.219941	0.185728	0.210166	0.234604	0.219941
12		0.219941	0.219941	0.219941	0.219941	0.219941	0.195503	0.210166	0.229717	0.219941
13		0.244379	0.244379	0.244379	0.244379	0.244379	0.200391	0.210166	0.215054	0.244379
14		0.249267	0.249267	0.249267	0.249267	0.249267	0.195503	0.229717	0.244379	0.249267
15		0.254154	0.254154	0.254154	0.254154	0.254154	0.190616	0.239492	0.244379	0.254154
16	2.5	0.361681	0.361681	0.361681	0.361681	0.361681	0.293255	0.312805	0.322581	0.361681
17		0.371457	0.371457	0.371457	0.371457	0.371457	0.327468	0.317693	0.337243	0.371457
18		0.371457	0.371457	0.371457	0.371457	0.371457	0.327468	0.347019	0.351906	0.371457
19		0.371457	0.371457	0.371457	0.371457	0.371457	0.332356	0.347019	0.376344	0.371457
20		0.351906	0.351906	0.351906	0.351906	0.351906	0.312805	0.342131	0.351906	0.351906
21		0.376344	0.376344	0.376344	0.376344	0.376344	0.312805	0.347019	0.356794	0.376344
22	3.0	0.469208	0.469208	0.469208	0.469208	0.469208	0.40567	0.464321	0.483871	0.469208
23		0.464321	0.464321	0.464321	0.464321	0.464321	0.42522	0.474096	0.464321	0.464321
24		0.464321	0.464321	0.464321	0.464321	0.464321	0.459433	0.449658	0.488759	0.464321
25		0.469208	0.469208	0.469208	0.469208	0.469208	0.439883	0.454545	0.469208	0.469208
26		0.469208	0.469208	0.469208	0.469208	0.469208	0.449658	0.483871	0.493646	0.469208
27		0.469208	0.469208	0.469208	0.469208	0.469208	0.44477	0.454545	0.469208	0.469208
28	3.5	0.552297	0.552297	0.552297	0.552297	0.552297	0.518084	0.56696	0.56696	0.552297
29		0.591398	0.591398	0.591398	0.591398	0.591398	0.552297	0.552297	0.576735	0.591398
30		0.576735	0.576735	0.576735	0.576735	0.576735	0.527859	0.557185	0.576735	0.576735
31		0.591398	0.591398	0.591398	0.591398	0.591398	0.527859	0.562072	0.58651	0.591398
32		0.581623	0.581623	0.581623	0.581623	0.581623	0.56696	0.58651	0.58651	0.581623
33		0.606061	0.606061	0.606061	0.606061	0.606061	0.537634	0.591398	0.581623	0.606061
34	4.0	0.7087	0.7087	0.7087	0.7087	0.7087	0.625611	0.674487	0.659824	0.7087
35		0.703812	0.703812	0.703812	0.703812	0.703812	0.654936	0.684262	0.679374	0.703812
36		0.698925	0.698925	0.698925	0.698925	0.698925	0.669599	0.659824	0.664712	0.698925
37		0.703812	0.703812	0.703812	0.703812	0.703812	0.659824	0.68915	0.664712	0.703812
38		0.723363	0.723363	0.723363	0.723363	0.723363	0.669599	0.694037	0.684262	0.723363
39		0.703812	0.703812	0.703812	0.703812	0.703812	0.674487	0.68915	0.669599	0.703812
40	4.5	0.777126	0.777126	0.777126	0.777126	0.777126	0.72825	0.777126	0.757576	0.777126
41		0.777126	0.777126	0.777126	0.777126	0.777126	0.747801	0.757576	0.786901	0.777126
42		0.811339	0.811339	0.811339	0.811339	0.811339	0.747801	0.786901	0.767351	0.811339
43		0.826002	0.826002	0.826002	0.826002	0.826002	0.733138	0.767351	0.772238	0.826002

44		0.806452	0.806452	0.806452	0.806452	0.806452	0.762463	0.767351	0.801564	0.806452
45		0.801564	0.801564	0.801564	0.801564	0.801564	0.738025	0.767351	0.801564	0.801564
46	5.0	0.840665	0.840665	0.840665	0.840665	0.840665	0.811339	0.835777	0.865103	0.840665
47		0.874878	0.874878	0.874878	0.874878	0.874878	0.840665	0.826002	0.860215	0.874878
48		0.855328	0.855328	0.855328	0.855328	0.855328	0.85044	0.826002	0.86999	0.855328
49		0.855328	0.855328	0.855328	0.855328	0.855328	0.83089	0.855328	0.865103	0.855328
50		0.889541	0.889541	0.889541	0.889541	0.889541	0.835777	0.85044	0.874878	0.889541
51		0.865103	0.865103	0.865103	0.865103	0.865103	0.826002	0.860215	0.879765	0.865103
52	5.5	0.904203	0.904203	0.904203	0.904203	0.904203	0.899316	0.899316	0.923754	0.904203
53		0.913978	0.913978	0.913978	0.913978	0.913978	0.884653	0.899316	0.899316	0.913978
54		0.913978	0.913978	0.913978	0.913978	0.913978	0.904203	0.899316	0.923754	0.913978
55		0.938416	0.938416	0.938416	0.938416	0.938416	0.889541	0.894428	0.904203	0.938416
56		0.918866	0.918866	0.918866	0.918866	0.918866	0.889541	0.894428	0.909091	0.918866
57		0.938416	0.938416	0.938416	0.938416	0.938416	0.889541	0.904203	0.938416	0.938416
58	6.0	0.957967	0.957967	0.957967	0.957967	0.957967	0.957967	0.943304	0.967742	0.957967
59		1.001955	1.001955	1.001955	1.001955	1.001955	0.933529	0.97263	0.97263	1.001955
60		1.016618	1.016618	1.016618	1.016618	1.016618	0.938416	0.977517	0.977517	1.016618
61		0.99218	0.99218	0.99218	0.99218	0.99218	0.962854	0.977517	0.997067	0.99218
62		1.016618	1.016618	1.016618	1.016618	1.016618	0.938416	0.97263	1.001955	1.016618
63		1.01173	1.01173	1.01173	1.01173	1.01173	0.97263	1.006843	1.001955	1.01173
64	6.5	1.050831	1.050831	1.050831	1.050831	1.050831	1.006843	1.016618	1.016618	1.050831
65		1.065494	1.065494	1.065494	1.065494	1.065494	1.036168	1.021505	1.050831	1.065494
66		1.075269	1.075269	1.075269	1.075269	1.075269	1.041056	1.026393	1.050831	1.075269
67		1.080156	1.080156	1.080156	1.080156	1.080156	1.036168	1.055718	1.026393	1.080156
68		1.050831	1.050831	1.050831	1.050831	1.050831	1.050831	1.026393	1.050831	1.050831
69		1.070381	1.070381	1.070381	1.070381	1.070381	1.021505	1.045943	1.031281	1.070381
70	7.0	1.109482	1.109482	1.109482	1.109482	1.109482	1.055718	1.104594	1.094819	1.109482
71		1.13392	1.13392	1.13392	1.13392	1.13392	1.060606	1.099707	1.085044	1.13392
72		1.13392	1.13392	1.13392	1.13392	1.13392	1.080156	1.085044	1.11437	1.13392
73		1.13392	1.13392	1.13392	1.13392	1.13392	1.089932	1.11437	1.104594	1.13392
74		1.13392	1.13392	1.13392	1.13392	1.13392	1.104594	1.089932	1.094819	1.13392
75		1.11437	1.11437	1.11437	1.11437	1.11437	1.099707	1.094819	1.124145	1.11437
76	7.5	1.13392	1.13392	1.13392	1.13392	1.13392	1.129032	1.11437	1.124145	1.13392
77		1.158358	1.158358	1.158358	1.158358	1.158358	1.138807	1.143695	1.124145	1.158358
78		1.138807	1.138807	1.138807	1.138807	1.138807	1.11437	1.138807	1.158358	1.138807
79		1.168133	1.168133	1.168133	1.168133	1.168133	1.11437	1.148583	1.158358	1.168133
80		1.143695	1.143695	1.143695	1.143695	1.143695	1.143695	1.129032	1.13392	1.143695
81		1.17302	1.17302	1.17302	1.17302	1.17302	1.148583	1.158358	1.13392	1.17302
82		1.17302	1.17302	1.17302	1.17302	1.17302	1.143695	1.158358	1.13392	1.17302
83		1.148583	1.148583	1.148583	1.148583	1.148583	1.143695	1.129032	1.15347	1.148583
84		1.168133	1.168133	1.168133	1.168133	1.168133	1.129032	1.13392	1.158358	1.168133

Calibration, Final Conclusions

Through optical observation of the graph of our experimental results, we can make a number of observations:

- There is a surprising repeatability of our measured results even for small load values;
- The force sensor actuated after a load of 1.5 N, a fact that agrees with our previous observations;
- The deviations remains relatively the same for different applied forces, a fact that contrasts our previous observations;
- The distinctive ability of the measurement system for loads bigger than 7 N is smaller than the distinctive error of our device;
- There is a recorded contribution of the dynamic nature of our device (viscoelastic nature of rubber discs, capacitors on the circuit) to the final measurements, but it is much smaller than the distinctive error of the device, and becomes irrelevant for steady or slowly developing loads;

According to the experimental results, the final suggested operational conditions are:

- Suggested Measured Range: **1.5 Newtons to 7 Newtons**
- The measured force equals to **F = 2.8677*V^2 + 1.871*V + 1.377 +/- 0.4 Newtons**, where V: the output of our system

The big measurement error of our device makes it inappropriate for precise measurements, although it can give us a good general approximation of the applied load on a surface or test specimens. Statistical approximations of large arrays of FSRs can give us a more detailed approximation of applied forces on specimens, but it still is far from an accurate method of force measurement. It is safe to say that the main contributor on this error is the FSR itself, although we have concluded that a more thorough mounting of the sensor can increase the precision of the measurements. The amplifying electronic circuit proved robust and precise with negligible noise although it's dynamic nature make it inappropriate for monitoring rapid changes of applied load.

References

Bibliography

1. Microelectronic Circuits (The Oxford Series in Electrical and Computer Engineering) [Adel S. Sedra, Kenneth C. Smith]
2. Βιομηχανικά Ηλεκτρονικά (Εκδόσεις ΕΜΠ) [Κυριακόπουλος Κωνσταντίνος]

Web sites

1. http://dlnmh9ip6v2uc.cloudfront.net/datasheets/Sensors/ForceFlex/2010-10-26-DataSheet-FSR400-Layout2.pdf
2. https://www.tekscan.com/product-group/embedded-sensing/force-sensors
3. http://electroforce.tainstruments.com/electroforce/en/web/3100_products/page.html
4. https://www.youtube.com/watch?v=K03Rom3Cs28
5. https://inst.eecs.berkeley.edu/~ee105/fa14/lectures/Lecture04-Non-ideal%20Op%20Amps%20(Feedback%20circuit).pdf
6. http://www.ti.com/general/docs/lit/getliterature.tsp?genericPartNumber=OPA4228&fileType=pdf
7. http://www.sensorwiki.org/doku.php/sensors/force-sensitive_resistor
8. http://www.ti.com/tool/tina-ti
9. http://www.linear.com/designtools/software/